BCI Control of Whole-body Simulated Humanoid by Combining Motor Imagery Detection and Autonomous Motion Planning

Karim Bouyarmane[1], Joris Vaillant[2,3], Norikazu Sugimoto[4], François Keith[2,3], Jun-ichiro Furukawa[1,5], and Jun Morimoto[1]

[1] ATR Computational Neuroscience Laboratories, Kyoto 619-0288, Japan
[2] CNRS-Montpellier 2 University LIRMM, 34000 Montpellier, France
[3] CNRS-AIST JRL, UMI3218/CRT, Tsukuba, Ibaraki 305-8568, Japan
[4] National Institute of Information and Communications Technology, Osaka 565-0871, Japan
[5] Osaka University, Osaka 565-0871, Japan.

Abstract. In this paper we demonstrate the coupling of an autonomous planning and control framework for whole-body humanoid motion, with a brain-computer interface (BCI) system in order to achieve online real-time biasing and correction of the offline planned motion. Using the contact-before-motion planning paradigm, the humanoid autonomously plans, in a first stage, its motion to reach a desired goal configuration or contact location. In the second stage of the approach, the humanoid executes the planned motion and the user can exert online some control on the motion being executed through an EEG decoding interface. The method is applied and demonstrated in a dynamics simulator with full collision-detection on a model of the humanoid robot HRP2.

Keywords: Humanoid Whole-Body Control, Motor Imagery BMI, Motion Planning

1 Introduction

Within humanoid robotics research, one natural question that immediately pops up in mind is the possibility of using the human brain motor functions to control the motion of a humanoid robot, the same way the human does to control the movements of their own body. This is basically the brain-machine interfacing (BMI) problem, with the "machine" here being instantiated as a humanoid robot, an intuitively natural hardware for implementing human brain motor control.

On the applicative side, brain-computer interface (BCI) systems provide promising perspectives for assistive applications directed towards motion-impaired users, enabling control of robotic prostheses or robotic assistants in daily-life tasks, among which humanoid-designed ones are of particular interest, since the non-expert user can easily be familiar with what to expect from a humanoid robot in terms of motion capabilities and general dexterity. Moreover, using legged humanoids allows to integrate them directly in a daily-life environment

that is designed for human activities and that accounts for human motion capabilities, without requiring to adapt the existing environment to the particular kinematics of the robot assistant.

These perspectives motivate our study. We propose to couple two components that appear necessary to reach these goals, namely a motion planning and control (MPC) framework for humanoid, with a non-invasive brain-signal measuring and decoding system. We base our study on state-of-the-art works that had been independently done on both ends, adapting them to allow their assembly as the two building blocks of the proposed integrated framework (Fig. 1).

This coupling of humanoid controller with BCI system has been achieved in previous works [1][2][3]. These works consider the problem from the following angle: the humanoid with its black-box walking controller (walking pattern generator) is seen as a mobile robot that can be commanded to walk forward, backward, or to turn right and left in a 2D plan (it can even be an actual mobile robot, ie. equipped with wheels rather than legs, in some of these works [4]), and the BCI command is generally generated through visual stimulation techniques (SSVEP [4][3][2] or P300 [1]).

We however chose to investigate alternative approaches from both ends. From the humanoid MPC end, we do not target cyclic walking motion, but general acyclic whole-body behaviours of which walking would be a particular instance. By doing so, we are able to take full profit of the dexterous capabilities of the humanoid design that initially motivate its use, for instance in climbing arbitrary-height stairs or using obstacles as contact support to reach the goal. We achieve this by exploiting our previously proposed multi-contact MPC paradigm for humanoids [5]. From the BCI end, we generate the command signal with motor imagery (MI) techniques rather than visual stimulation, which constitute the state of the art in non-invasive BCI. In the present work, the MI decoding technique that we adapted from previous application on the control of one-DOF robot and of standing-up/sitting-down motion of exoskeleton [6] allows to generate a three-valued discrete command for a one-dimensional feature of the whole-body motion, in this case the motion along a generalized notion of "vertical axis" of the moving end-limb, such as the foot of the swing leg in a biped motion for instance. However we believe, from recent and ongoing studies, that the MI approach can in the near future enable the control of a two-dimensional continuous feature of the motion [7][8].

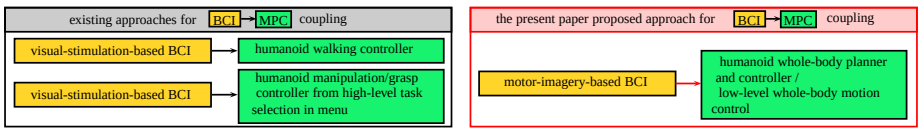

Fig. 1: Overview of the two-component coupling framework

The rest of this paper is organized as follows. The two components of the framework, the MPC scheme for the humanoid, and the MI BCI decoding scheme, are respectively recalled in sections 2 and 3, section 4 presents the strategy we retained for coupled exploitation of these components in our applicative perspective, and section 5 comments an illustrative experiment. Finally section 6 concludes the paper.

2 Humanoid Whole-Body Motion Planning and Control

We recall our work on humanoid MPC [5]. The aim here is to autonomously generate a whole-body motion of the humanoid that realises a desired task, thus sparing the user the tedious task of designing the high-DOF motion and allowing high-level (task-level) control, in line with state-of-the-art BCI capabilities.

Note that we do not make a priori assumption on the nature of the motion, e.g. cyclic walking, and thus the planning does not occur at path planning level for a walking robot, nor at footstep planning level for an a priori biped motion [9][10][11] but rather at the high-dimensional configuration space level of whole-body humanoid motion, including the free-floating component. Classic approaches operating at this level for humanoids adapted randomized planning techniques considering the humanoid with fixed foot locations as the fixed root of its kinematic tree [12][13][14][15]. Our approach merges these two planning levels (footstep planning for cyclic walking, whole-body motion on fixed foot locations) and is classified within the contact-before-motion planning category [16]. The motion generation is done in two stages.

First, planning offline the sequence of changes in *contact state* with the environment, each of which is associated with an inverse-kinematics realizing configuration [17]. By running a greedy best-first search algorithm on all possible pairings (contacts) between a robot link surface and an environment surface to be added or removed to the contact state being explored, we obtain our sequence. See details in [18][5].

In the second stage, an online controller tracks successively each of these intermediate postures (called a *step*), removing or adding a contact at each step. It is formulated as a Quadratic Program (QP) optimization problem with weighted tasks that are defined according to a finite-state machine (FSM) consisting of two states: "Move CoM" state when removing a contact from the current stance, and"Move Contact Link" state when adding a contact to the current stance. See [19] for the detailed formulation of the QP and FSM states.

3 BCI decoding

As non-invasive brain signal acquisition device we used an EEG system (64 channels and sampling rate of 2048 Hz). The brain signals are decoded and classified using the method applied and presented in the previous work [6], based on the spectral regularization matrix classifier [20][21], that we recall here.

The EEG signals, of covariance matrices $\mathbf{C}$ considered as input, are classified into two classes, labelled with the variable k, with respective output probabilities (at sampled time t): $P(k_t = +1|\mathbf{C}_t) = \frac{1}{1+\exp(-a_t)}$, and $P(k_t = -1|\mathbf{C}_t) = \frac{\exp(-a_t)}{1+\exp(-a_t)}$, with $a_t = \mathrm{tr}[\mathbf{W}^\top \mathbf{C}_t] + b$, and where $\mathbf{W}$ is the parameter matrix to be learned (b is a constant-valued bias).

To learn $\mathbf{W}$ the minimization problem $\min \sum_{t=1}^{n} \ln(1+\exp(-k_t a_t)) + \lambda \|\mathbf{W}\|_1$, is solved, λ being the regularization variable ($\lambda = 14$ in the application below) and $\|\mathbf{W}\|_1 = \sum_{i=1}^{r} \sigma_i[\mathbf{W}]$ being the spectral l_1-norm of $\mathbf{W}$ (r is the rank of $\mathbf{W}$ and $\sigma_i[\mathbf{W}]$ its i-th singular value).

Once the classifier learned, the 7-30 Hz band-pass-filtered measured EEG signals are decoded online, by down-sampling them from 2048 Hz to 128 Hz, and applying Lapace filtering and common average substraction to remove voltage bias. Their covariance matrix, initialized at $\mathbf{C}_t = \mathbf{x}_t^\top \mathbf{x}_t$ for the first time step $t = 1$, where $\mathbf{x}_t \in \mathbb{R}^{1\times 64}$ denotes the filtered EEG signals, are updated at every time step following $\mathbf{C}_t = \frac{1}{N}\mathbf{x}_t^\top \mathbf{x}_t + \frac{N-1}{N}\mathbf{C}_{t-1}$, and used to compute the classification probabilities above.

Finally, the three-valued discrete command c_t that is sent to the robot is selected from these probabilities through the following hysteresis ($P_{\mathrm{thresh}} = 0.6$)

$$c_t = \begin{cases} +1 & \text{if } P(k_t = +1|\mathbf{C}_t) > P_{\mathrm{thresh}} \text{ and } c_{t-1} \neq +1\,, \\ -1 & \text{if } P(k_t = -1|\mathbf{C}_t) > P_{\mathrm{thresh}} \text{ and } c_{t-1} \neq -1\,, \\ 0 & \text{otherwise}\,. \end{cases} \tag{1}$$

4 Coupling the two components

The command c_t devised in Eq. (1) is sent to the online humanoid whole-body controller via UDP protocol at 128 Hz frequency and used to modify the planned and autonomously executed motion of the humanoid robot as described below.

When the robot is executing a step that requires moving a link to a planned contact location (state"Move Contact Link" of the FSM), then instead of tracking directly the goal contact location, we decompose the motion of the the contact link into two phases: a lift-off phase in which the link first tracks an intermediate position located at a designated way-point, followed by a touch-down phase in which the link tracks its final goal location in the contact sequence. This two-phase decomposition allows the link to avoid unnecessary friction with the environment contact surface and to avoid colliding with environment features such as stairs. Each of these two phases correspond to a sub-state of the meta-state "Move Contact Link" of the FSM, namely "Go to Way-point" and "Go to Goal" states. Finally, in order to avoid stopping the motion of the contact link at the way-point and to ensure a smooth motion throughout the step, the transition between the two sub-states is triggered when the contact link crosses a threshold plan before reaching the tracked way-point. For clarity of the presentation we will not go into this detail.

A default position of the intermediate way-point is automatically pre-set by the autonomous framework using the following heuristic: Let P_s and P_g denote

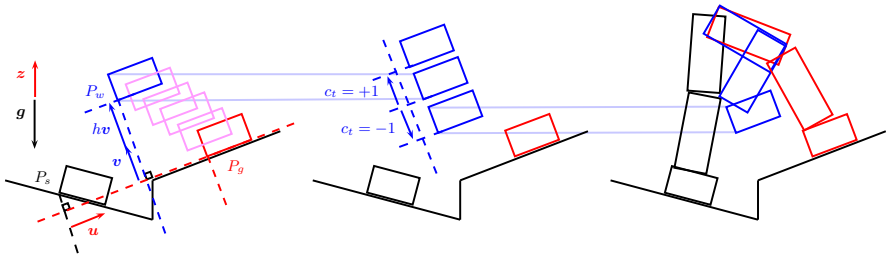

Fig. 2: Way-point moving strategy. Only the swing foot is represented. In black its initial position at the beginning of the step, in red its target final position as planned at the end of the step, in blue its way-point position at mid-step. Left: a default position is set for the way-point based on its final position. Middle: by sending the command c_t the user can bring up or down the position of the way point (in this case down). Right: the resulting executed motion of the swing leg.

respectively the step start and goal positions of the contact link, $\boldsymbol{g}$ the gravity vector, $\boldsymbol{z} = -\boldsymbol{g}/\|\boldsymbol{g}\|$ the unit vector opposite to $\boldsymbol{g}$, and $\boldsymbol{u} = \overrightarrow{P_s P_g}/\|\overrightarrow{P_s P_g}\|$ the unit vector from P_s to P_g. Finally let $\boldsymbol{v} = \boldsymbol{u} \times (\boldsymbol{z} \times \boldsymbol{u})$ be the unit vector normal to $\boldsymbol{u}$ and in the plan defined by $\boldsymbol{u}$ and $\boldsymbol{z}$. The way-point P_w is defined as (see Fig. 2) $P_w = P_g - \frac{1}{2}\overrightarrow{P_s P_g} + h\,\boldsymbol{v}$, where h is the hand-tuned user-defined parameter that specifies the height of the steps. The command c_t that comes from BCI decoding system is finally used to modify in real-time this way-point position P_w by modifying its height h. Let δh denote a desired height control resolution, then the modified position of the way-point through the brain command c_t becomes

$$P_w(c_t) = \begin{cases} P_g - \frac{1}{2}\overrightarrow{P_s P_g} + (h + c_t\,\delta h)\,\boldsymbol{v} & \text{if } t = 1\,, \\ P_w(c_{t-1}) + c_t\,\delta h\,\boldsymbol{v} & \text{if } t > 1\,. \end{cases} \tag{2}$$

The command c_t could have been used in other ways, however two principles should stand in any BCI low-level control of humanoid motion 1) the full detailed motion, that cannot be designed joint-wise by the BCI user, should be autonomously planned and executed from high-level (task-level) command, and 2) the brain command can then be used to locally correct or bias the autonomously planned and executed motion. The way-point is a key-feature to be controlled according to these two principles as it helps overcome the shortcomings of the autonomous collision-avoidance constraint in the QP controller. This collision-avoidance constraint acts as a repulsive field when the way-point of the link acts as an attracting field of the contact link. The resultant field can display local extrema corresponding to equilibrium situations in which the link stops moving though without completing its tracking task. Manual user intervention, here through the brain command, is then necessary to un-block the motion of the link by moving the way-point. The brain command is thus used for low-level correction of the inherent limitations of autonomous planning endeavours.

5 Illustrative Experiment

We describe now the experiment we designed (Fig. 3, left) (and illustrative video which can be downloaded at `www.cns.atr.jp/~karim/iconip2013.wmv`).

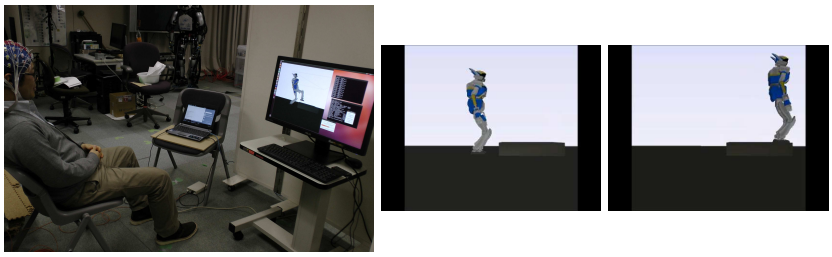

Fig. 3: Left: Experiment setup. Right: Initial and goal configurations.

An initial and goal configurations are pre-specified manually by the user among a finite number of locations in the environment (Fig. 3, right). In this case the initial configuration is standing in front of a stair and the goal task is to go up on the stair. This selection is for now done manually, but it can later be selected also through a brain command by embedding the strategy described in this work within a hierarchical framework such as in [3][4], that will switch between the behaviour of selecting the high-level goal task and the low-level motion control. Offline, the framework autonomously plans the transition sequence (Fig. 4), then the online controller is executed (Fig. 5).

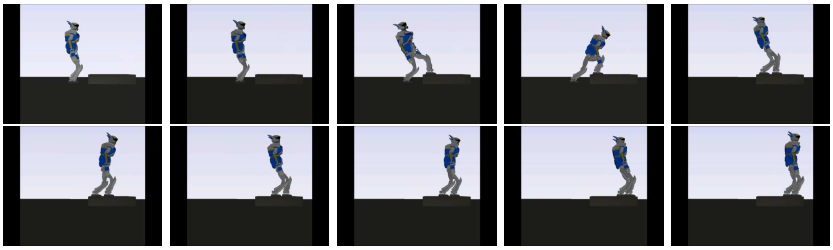

Fig. 4: The autonomously offline planned sequence of intermediate static configurations. The second posture removes the left foot contact from the stance by shifting all the weight on the right foot support. The third posture moves the now support-free left foot and adds it to the stance, etc.

The user wears an EEG cap and is trained with 3 training sessions of approximately 5 min each to learn the parameter of the classifier, through a MI task consisting of imagining respectively left arm and right arm movements for going

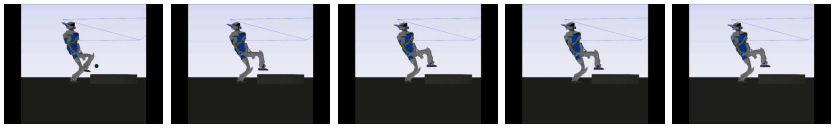

Fig. 5: Tracking the BCI-controlled way-point, ie. the user controlled motion: in the extreme left figure the small black sphere in front of the swing foot indicates the way-point position that the user can control. When the swing foot reaches the black sphere (second figure) it keeps following it according to the user commands (go up or down) in the subsequent figures (up then down then up).

up and down. The user has visual feed-back from the simulator on the desktop computer screen. The decoding of the BCI command is done in real-time and implemented in Matlab, and the brain command is then sent via UDP protocol to the dynamics simulator process implemented in C++.

We tested the way-point control strategy in the second step of the motion (the first contact-adding step along the sequence). The user controlled the position of a black sphere that represents the way-point tracked by the foot of the robot in real-time, while autonomously keeping balance and avoiding self-collisions, joint limits, and collision with the environment. We then externally (manually) triggered the FSM transition to the following step and left the autonomous controller complete the motion without brain control. See the video.

Fig. 6 illustrates the control performances of the BCI decoder. Table 1 gives computation time figures executed on a Dell Precision T7600 Workstation equipped with a Xeon processor E5-2687W (3.1GHz, 20M).

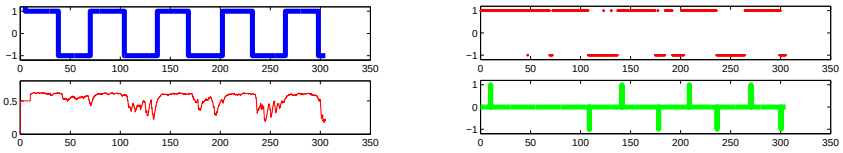

Fig. 6: BCI decoding performances. On the horizontal axis is step number t. From top to bottom and left to right: the command cue in thick blue, the decoded brain activities ($P(k_t = +1|\mathbf{C}_t)$) in thin red, the probability 0.5 thresholded estimated classified label (ie. $P(k_t = +1|\mathbf{C}_t) \geq 0.5$ or < 0.5) in thick red point marker, the command c_t sent to the robot (based on the threshold $P_{\text{thres}} = 0.6$) in thick green.

From this experiment, we confirmed that the MPC framework can be coupled with the BCI decoding system in real-time and that the robot can safely realize the task while receiving and executing the brain command.

Offline planning	2.7sec
Average online control command (QP) (@ 200Hz)	2.661ms
Average online simulation step (@ 1kHz)	0.389ms
BCI classifier training and learning session	$\sim$ 30min
Average online BCI signal buffering (@ 2048Hz)	0.137ms
Avg online BCI classification (@ 128Hz) no control signal sent ($c_t = 0$)	0.204ms
Avg BCI classification (@ 128Hz) control signal sent ($c_t = +1$ or -1)	6.20ms

Table 1: Execution time figures (not including OpenGL rendering time)

6 Discussion and Future Work

This work demonstrated the technical possibility of real-time online low-level control of whole-body humanoid motion using motor-imagery-based BCI.

We achieved it by coupling an existing EEG decoder and whole-body multi-contact acyclic planning and control framework. This coupling allowed us to control a one-dimensional feature of the high-DOF whole-body motion, designed as the generalized height of moving link way-point, in a discrete way.

We aim now at continuous control of two-dimensional feature of this whole-body motion, allowing not only the control of the tracked way point but also of a corresponding threshold plan that decides when to trigger the transition between the lift-off and touch-down phases. We believe this can be achieved based on the previous work done for example on two-dimensional cursor control [7].

Finally, we aim at porting this framework from the simulation environment to the real robot control.

Acknowledgments. This work is supported with a JSPS Postodoctoral Fellowship for Foreign Researchers, ID No. P12707. A part of this study is the result of Brain Machine Interface Development carried out under the Strategic Research Program for Brain Sciences by the Ministry of Education, Culture, Sports, Science and Technology (MEXT) of Japan. J.M. was partially supported by MEXT KAKENHI Grant Number 23120004 and by Strategic International Cooperative Program, JST. J.V. and F.K. were partially suported by grants from the RoboHow.Cog FP7 `www.robohow.eu`, Contract N288533. The authors would like to thank Abderrahmane Kheddar for valuable use of the AMELIF dynamics simulation framework.

References

1. C. J. Bell, P. Shenoy, R. Chalodhorn, and R. P. N. Rao. Control of a humanoid robot by a noninvasive brain-computer interface in humans. *Journal of Neural Engineering*, 5:214–220, 2008.
2. P. Gergondet, S. Druon, A. Kheddar, C. Hintermuller, C. Guger, and M. Slater. Using Brain-Computer Interface to Steer a Humanoid Robot. In *IEEE International Conference on Robotics and Biomimetics*, pages 192–197, Phuket, Thailand, 2011.

3. M. Chung, W. Cheung, R. Scherer, and R. P. N. Rao. A Hierarchical Architecture for Adaptive Brain-Computer Interfacing. In *Proceedings of the Twenty-Second international joint conference on Artificial Intelligence - Volume Two*, pages 1647–1652, 2011.
4. M. Bryan, J. Green, M. Chung, L. Chang, R. Scherery, J. Smith, and R. P. N. Rao. An Adaptive Brain-Computer Interface for Humanoid Robot Control. In *11th IEEE-RAS International Conference on Humanoid Robots*, pages 199–204, Bled, Slovenia, 2011.
5. K. Bouyarmane and A. Kheddar. Humanoid robot locomotion and manipulation step planning. *Advanced Robotics*, 26(10), 2012.
6. T. Noda, N. Sugimoto, J. Furukawa, M. Sato, S. Hyon, and J. Morimoto. Brain-controlled exoskeleton robot for bmi rehabilitation. In *12th IEEE-RAS International Conference on Humanoid Robots*, pages 21–27, Osaka, Japan, 2012.
7. J. R. Wolpaw and D. J. McFarland. Control of a two-dimensional movement signal by a noninvasive brain-computer interface in humans. *Proceedings of the National Academy of Sciences*, 101(51):17849–17854, 2004.
8. K. J. Miller, G. Schalk, E. E. Fetza, M. den Nijs, J.G. Ojemanne, and R.P.N. Rao. Cortical activity during motor execution, motor imagery, and imagery-based online feedback. *Proceedings of the National Academy of Sciences*, 2010.
9. J.J. Kuffner, K. Nishiwaki, S. Kagami, M. Inaba, and H. Inoue. Footstep Planning Among Obstacles for Biped Robots. In *IEEE/RSJ International Conference on Intelligent Robots and Systems - Volume 1*, pages 500–505, Maui, HI, 2001.
10. J. Chestnutt, J. Kuffner, K. Nishiwaki, and S. Kagami. Planning Biped Navigation Strategies in Complex Environments. In *IEEE-RAS International Conference on Humanoid Robots*, Munich, Germany, 2003.
11. J. Chestnutt, M. Lau, J.J. Kuffner, G. Cheung, J. Hodgins, and T. Kanade. Footstep Planning for the ASIMO Humanoid Robot. In *IEEE International Conference on Robotics and Automation*, pages 629–634, Barcelona, Spain, 2005.
12. J.J. Kuffner, S. Kagami, K. Nishiwaki, M. Inaba, and H. Inoue. Dynamically-Stable Motion Planning for Humanoid Robots. *Autonomous Robots*, 12:105–118, 2002.
13. Katsu Yamane, James Kuffner, and Jessica K Hodgins. Synthesizing Animations of Human Manipulation Tasks. *ACM Transactions on Graphics (Proc. SIGGRAPH 2004)*, 23(3), August 2004.
14. E. Yoshida, O. Kanoun, C. Esteves, and J. P. Laumond. Task-driven Support Polygon Reshaping for Humanoids. In *6th IEEE-RAS International Conference on Humanoid Robots*, pages 208–213, Genova, Italy, 2006.
15. Eiichi Yoshida, Jean-Paul Laumond, Claudia Esteves, Oussama Kanoun, Takeshi Sakaguchi, and Kazuhito Yokoi. Whole-body locomotion, manipulation and reaching for humanoids. In Arjan Egges, Arno Kamphuis, and Mark Overmars, editors, *Motion in Games*, volume 5277 of *LNCS*, pages 210–221. Springer Berlin Heidelberg, 2008.
16. K. Hauser, T. Bretl, J.-C. Latombe, K. Harada, and B. Wilcox. Motion Planning for legged Robots on Varied Terrain. *International Journal of Robotics Research*, 27(11-12):1325–1349, November-December 2008.
17. K. Bouyarmane and A. Kheddar. Static multi-contact inverse problem for multiple humanoid robots and manipulated objects. In *10th IEEE-RAS International Conference on Humanoid Robots*, pages 8–13, Nashville, TN, 2010.
18. K. Bouyarmane and A. Kheddar. Multi-contact stances planning for multiple agents. In *IEEE International Conference on Robotics and Automation*, pages 5546–5353, Shanghai, China, 2011.

19. K. Bouyarmane and A. Kheddar. Using a multi-objective controller to synthesize simulated humanoid robot motion with changing contact configurations. In *IEEE/RSJ International Conference on Intelligent Robots and Systems*, pages 4414–4419, San Fransisco, 2011.
20. R. Tomioka and K. Aihara. Classifying matrices with a spectral regularization. In *24th international conference on Machine learning*, pages 895–902, New York, 2007.
21. R. Tomioka and K.R. Muller. A regularized discriminative framework for EEG analysis with application to brain-computer interface. *NeuroImage*, 49:415432, 2010.